UPPSALA
UNIVERSITET

UPTEC E 18 002
Examensarbete 30 hp
Februari 2018

Construction, testing and verification of a brushless excitation system with wireless control of the field current in a synchronous generator

Rickard Larsson
Kenny Andersson

UPPSALA
UNIVERSITET

Teknisk- naturvetenskaplig fakultet
UTH-enheten

Besöksadress:
Ångströmlaboratoriet
Lägerhyddsvägen 1
Hus 4, Plan 0

Postadress:
Box 536
751 21 Uppsala

Telefon:
018 – 471 30 03

Telefax:
018 – 471 30 00

Hemsida:
http://www.teknat.uu.se/student

Abstract

Construction, testing and verification of a brushless excitation system with wireless control of the field current in a synchronous generator

Rickard Larsson, Kenny Andersson

Synchronous generators have been used in hydropower from more than a century where, traditionally, the field current is transferred to the rotor using slip rings and carbon brushes. There are some major disadvantages following the use static excitation; regular and expensive maintenance, as well as a source of carbon dust which, due to buildup, may cause short circuits. To avoid these problems associated with slip ring exciter systems, a system that use induction to transfer power to the rotor could be used instead.

Systems that utilize brushless excitation today usually regulates the current by controlling the magnetization of the exciter stator, which is comparably slower than their static counterparts. In order to allow for swift regulation of the field current from a brushless exciter, required power electronics and controllers have to be present on the rotor shaft instead. The aim of this project is to start investigating if commercially available products, which are originally indented to be used in a stationary environment, could accomplish this.

The results from this study shows that it is possible to use such products to control the field current. The components were found to withstand the exposure of high g-forces and vibrations, albeit only during the relatively small amount of time in which rotary testing was performed. As such there is no certainty that the components would remain functional for the considerably longer time that any commercial use would require them to.

Handledare: Eyuel Tibebu
Ämnesgranskare: Urban Lundin
Examinator: Tomas Nygren
ISSN: 1654-7616, UPTEC E 18 002

Acknowledgementes

We would like to give our sincere thanks to Mats Wahlén and our supervisor Eyuel Tibebu at Svea Power for giving us this opportunity to work with something we found very intriguing and for all the support along the way.

We would also like to thank our reviewer Urban Lundin as well as Fredrik Evestedt and Jose Perez at Uppsala University for their guidance during this project.

Svensk Sammanfattning

Synkrongeneratorer har använts inom vattenkraft sedan lång tid tillbaka där rotorn traditionellt sett magnetiseras med hjälp av släpringar och kolborstar. Användning av denna typ av magnetisering medför däremot stora kostnader och problem gällande underhåll då kolborstarna slits ner och sprider koldamm, som i värsta fall kan orsaka en kortslutning. Dessa problem kan dock undvikas genom att frångå matning genom direktkontakt och istället överföra energin med hjälp av induktion, så kallade borstlösa matare.

Magnetiseringssystem som använder sig av konventionell borstlös matning styr rotorströmmen genom att reglera magnetiseringen av matarstatorn där endast passiv likriktning sker på den roterande sidan. Den sortens styrning är vanligtvis långsammare än styrningen av statisk magnetisering. För snabb reglering av rotorströmmen vid borstlös matning krävs därför placering av aktiv kraftelektronik samt styrsystem på rotoraxeln. Vårt uppdrag är att påbörja en undersökning om kommersiella produkter som ursprungligen är gjorda för att sitta i en stationär miljö kan utföra detta.

Resultatet från denna rapport visar på att det är möjligt att använda denna typ av produkter för att styra rotorströmmen. Komponenterna klarade av påfrestningarna från g-krafterna såväl som vibrationerna, om än bara under den relativt korta tiden som de roterande testerna utfördes. Således finns det inga garantier att komponenterna kommer att bibehålla sin funktionalitet under den betydligt längre tid som vid kommersiell användning skulle krävas.

Abbreviations

DC	Direct Current
AC	Alternating Current
PM	Permanent Magnet
BT	Bluetooth
FHSS	Frequency-Hopping Spread Spectrum
PID	Proportional-Integral-Derivative
SCR	Silicon Controlled Rectifier
PLL	Phase Locked Loop
I/O	Input/Output
SE	Structural Enclosure
RPM	Revolutions Per Minute
GUI	Graphical User Interface

Contents

1 Introduction

Synchronous generators have been used for more than a century and is today a very integral part of any power grid. These machines are responsible for converting the mechanical energy produced by a turbine to electrical energy that can be transferred over the grid. The use of synchronous generators are predominant in hydro-power where they are also used to stabilize the grid as regulation capacity against load variations and intermittent power sources. The large size of such generators also means that their inertia cancels out smaller, and faster, frequency fluctuations on the grid.

In order to balance the grid both active and reactive power has to be maintained and this is where the excitation system is important. By increasing the current through the field windings of the rotor the generator can act as a source of reactive power whenever it is needed, while reducing it allows for the generator to absorb reactive power. Adjusting the field current is also one way to keep the output voltages stable.

Traditionally excitation of the rotor is done by applying a direct current (DC) on the field winding, through slip rings, with the use of carbon brushes. Advantages of such a solution includes fast step response which is crucial for regulating purposes and is therefore still the main system being used on large hydro power generators. On the other hand the maintenance needed is high as the carbon brushes are in physical contact with the rotating slip rings, this leads to wear and tear, causing deposits of carbon dust to build up in the generator, which ultimately could lead to short circuits. Brushless excitation solves this problem as there is no galvanic contact between the stationary and rotating sides. Such an exciter could generally be described as an outer pole generator, that is attached to the same shaft as the main generator, with its output on the rotating side. The produced alternating current (AC) is then rectified and used to magnetize the field windings of the main generator.

Conventional rotating exciters using a diode bridge are usually considered less attractive than their stationary counterparts due to a comparably slow response time, restricting regulatory capabilities of the generator.

This problem arise from the fact that there is no direct control on the rotating side of the exciter and that a negative field voltage for fast de-excitation cannot be applied. One solution which has been put forth is the use of a wirelessly controlled thyristor bridge, indeed proving that brushless excitation with a fast response time is possible. However such a solution is today very tailor-made and expensive.

1.1 Project background

Swedish Electrical and Power Control AB, SVEA Power for short, want to study the possibility of creating a 12-pulse excitation system for use in the high g-force environment caused by turning of a rotor.

This project is being done in collaboration with the Division of Electricity at Uppsala University, and as such testing will ultimately be done using an experimental generator called SVANTE. The test rig is a salient pole synchronous generator equipped with a brushless exciter that can be configured to produce either 3 or 6 phases for use in 6- or 12-pulse rectifying respectively.

Physical and electrical specifications of SVANTE can be seen in table 1. Furthermore an overview of the generator is shown in fig.1.

Parameter	Value
Frequency	50Hz
Number of pole pairs	6
Speed	500rpm
Slots per pole and phase	3
Number of stator slots	108
Coil pitch	9
Stator inner diameter	725mm
Stator length	303mm
Air gap length	8.4mm
Power of driving motor	75kW
Rotor weight	900kg
Stator weight	700kg

Table 1: Electrical and physical properties[1].

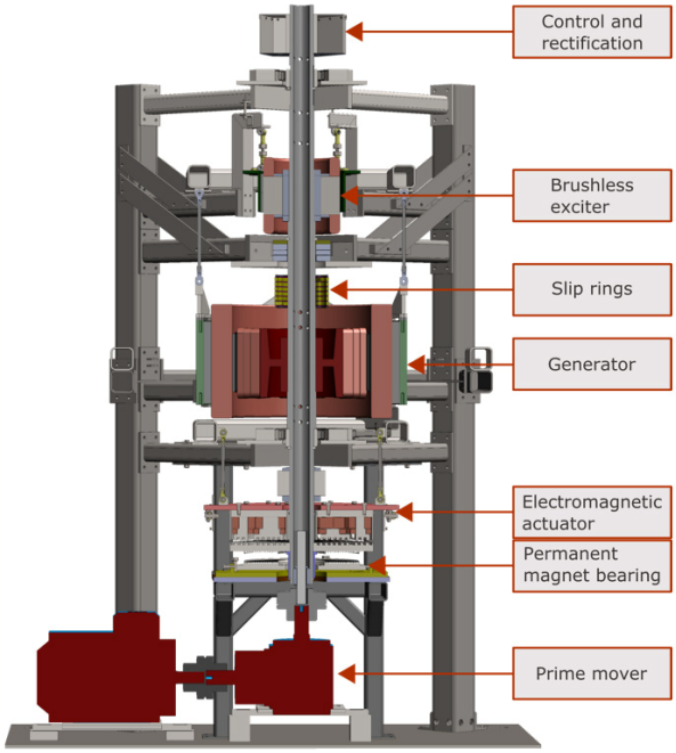

Figure 1: CAD drawing of the test rig.

1.2 Project description

This project aims to study the possibility of creating a part of an excitation system from commercially available products, not originally intended for use in a rotating environment, in order to bring down both cost and complexity of creating such a system.

Initially, stationary testing and designing of the system will be done simultaneously in order to optimize and verify desired functionality before preparing it for rotational tests. Preparation of the system includes assembly of the components inside a structural enclosure to be placed on top of the generator shaft, additional system functionality testing and finally mounting the whole system to the generator.

During rotational testing the system will be exposed to both high g-forces and vibrations that might damage the components. Therefore the rotating tests will start at a low speed that will be incrementally increased towards nominal speed, monitoring the system functionality continuously.

For the system to be considered functional it will have to fulfill the requirements stated below:

- Fully functional 12-pulse rectifying using thyristors.
- Wireless transmission of analog and digital signal used for control and monitoring.
- Rotating system being galvanically separated from the stationary side.
- Retained system functionality during and after rotating tests.
- Ability of applying negative field voltage on the rotor winding for faster regulation of the excitation current.

If system functionality is retained during rotation, measurements of the vibrations stemming from torque pulsation will be measured and analyzed during both 6- and 12-pulse rectifying.

2 Theory

2.1 Synchronous generators

Synchronous generators are machines used for the purpose of converting mechanical energy into electrical energy[2]. The rotor in such a machine is usually built as an electromagnet where the rotor magnetic field is produced from a DC current in the rotor winding, i.e. field current. The stator is in turn built using magnetically conductive material as a backbone in order to reduce reluctance and guide the magnetic flux around the stator windings. The windings are separated into three circuits, producing three phases of output with equal voltage and frequency, where each phase is shifted 120 electrical degrees from one another.

Turning of the rotor is achieved by applying a torque on the shaft, either from a turbine or a motor, creating a rotating magnetic field inside the generator. This magnetic field, which is constantly changing from the perspective of the stator windings, induces a voltage in each of the stator windings proportional to the strength of the magnetic field, ϕ, and rate of rotation in radians per second, ω.

$$E_s = K\phi\omega \tag{1}$$

Where K is a constant derived form the physical properties of the machine.

As per definition the electrical frequency of the produced voltage in a synchronous generator is locked to its mechanical rate of rotation. And when coupled to the grid, the electrical frequency dictates this mechanical rate of rotation in accordance with Eq. 2:

$$n_m = \frac{120 f_e}{P} \tag{2}$$

Where f_e is the electrical frequency in Hz, n_m the mechanical rotation of the rotor in revolutions per minute and P the number of poles.

2.2 Brushless excitation

Excitation of the rotor is a very integral part of every synchronous generator not using permanent magnets. As previously explained this is achieved by passing a DC current through the rotor winding which usually stems from a source separate to the generator itself, transferred over to the rotor using slip rings and carbon brushes.

Brushless excitation, however, works by using a smaller generator, with its rotor on the same shaft as the main rotor, to produce the current needed for excitation. The rotating exciter is essentially a generator with its outputs on the rotating side instead, bypassing the need for a galvanic interface between the rotating and stationary sections. The induced AC voltage then needs to be rectified before being fed to the rotor winding.

For the purpose of lowering torque pulsation[3] and DC voltage ripple a rotating exciter can be designed to produce a six-phase output, thus allowing for the utilization of twelve-pulse rectification. Furthermore, the use of brushless excitation with controllable power electronics on the rotor shaft increases the fault ride-through capability of a generator, allowing for a higher nominal power rating than previously possible due to safety margin restrictions[4].

2.3 The thyristor

The thyristor is a solid-state semiconductor device that can be operated in two modes, either inhibiting or allowing the conduction of current from anode to cathode. The state in which it operates is controlled by applying a signal to its gate. Whenever the signal amplitude exceeds a certain threshold in terms of voltage and current it will start conducting, where it will keep on conducting even if the signal were to be removed, and will do so until the primary current through it reaches zero. As with simple diodes the thyristor also blocks current from flowing in reverse, i.e. from cathode to anode, even when a signal is applied to its gate.

Further properties of the thyristor includes comparably high power ratings and non-proportional IV characteristics, meaning that it only operates in fully conducting or non-conducting mode, making it suitable as a switch.

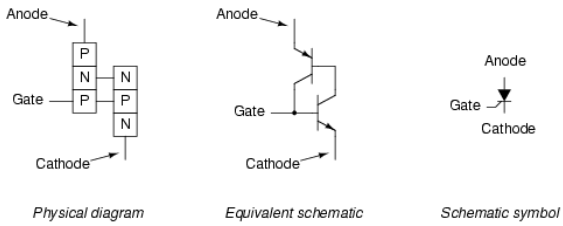

Figure 2: Physical diagram, schematic and symbol of the thyristor[5].

Physically the thyristor is built up of four layers of alternating P- and N-doped semiconductor material as seen in fig 2. It is essentially two transistors in a positive feedback loop, each feeding the gate of the other one, thus removing the need for further external signals to keep on conducting.

2.3.1 Bridge rectifier

With the use of six (or more) passive or active semiconductor devices arranged in a bridge configuration a three-phase AC input can be converted to a DC output. When using diodes in this configuration it is considered a passive bridge rectifier which is the simplest implementation of this technology. In such a scenario rectifying of the input happens automatically whenever a pair of diodes becomes forward-biased. For more controllability of this process the diodes are replaced with thyristors, where they not only need to be forward-biased but also, as stated earlier, supplied with a firing signal to the gate terminal in order to start conducting. Such a topology can be seen in fig 3 below.

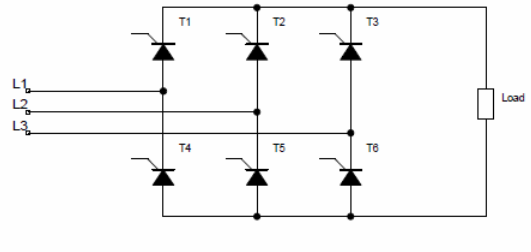

Figure 3: Three-phase bridge rectifier using thyristors.

By using a thyristor based solution the DC voltage and current can be controlled by changing the firing angle of the signal being applied to the thyristors. The firing angle dictates a delay in electrical degrees, after voltage crossover, before the firing signal is sent to the thyristor. In the example below a firing angle of 15 degrees has been specified which is clearly seen in the load voltage.

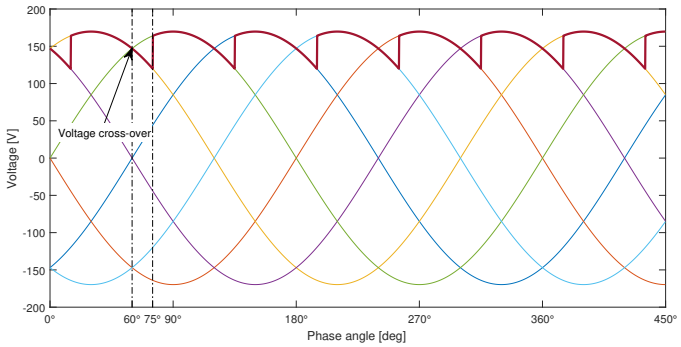

Figure 4: Voltages over each thyristor and load with a 15 degree firing angle.

2.4 Bluetooth

Bluetooth (BT) as an industry standard began in 1998 when Ericsson, IBM, Intel, Nokia, and Toshiba started the Bluetooth Special Industry Group (SIG). Their collaboration resulted in a global solution for communication in the unlicensed 2.4GHz ISM (industrial, scientific and medical) band for short range wireless devices and was made to replace cables between electronic devices.[6]

One of the features with BT is that it uses a frequency hop transceiver to reduce interference and fading and provides many FHSS (Frequency-hopping spread spectrum) carriers. There are two different types of BT systems, the first is Basic Rate and the other is Low Energy. The Basic Rate version has the option to use Enhanced Data Rate and the Low Energy version has lower current consumption and is overall less complex and thereby reduces the cost of the device. Basic rate and Low Energy supports a bit rate of 1 Megabit per second while Enhanced Data Rate can go up to 2 or 3 Megabit per second.

The connection between the Basic Rate BT devises is established by radio channel with a specific frequency hopping pattern and a common clock. One of the devices connected provides a synchronization reference and is called a master, the other devices connected are called slaves.[7]

2.5 Hall effect measurement

In order to regulate apparent output power from a generator there needs to be continuous measurements of the rotor field current such that it can be used as a regulating parameter. For high power applications one suitable current measurement technique is the hall effect measurement technique. It utilizes the magnetic flux created by the current in a conductor by concentrating it a magnetic circuit with a small airgap. In the airgap the hall voltage can be measured with a hall element by means of the Lorentz force. This force essentially deflects passing electrons proportionally to the magnetic flux density, and by extension the primary current. The hall voltage is then amplified and conditioned to provide an instantaneous measurement of the primary current.

2.6 Torque pulsation

Torque pulsation (torque ripple) is the variations in torque from the rotor that causes unwanted vibrations. These vibrations slowly wears down the generator which leads to higher maintenance and more downtime. [8] One of the many reasons why this occurs is related to the fundamental frequency of induced voltages in the exciter. For a 6-pulse system the frequency of the torque pulsations will be six times this fundamental frequency and twelve times for a 12-pulse system. [3]

On way to calculate the torque ripple is with the peak to peak torque difference divided by the average torque shown in eq.3. [8]

$$T_{ripple} = \frac{T_{max} - T_{min}}{T_{avg}} * 100 \tag{3}$$

3 Method

In this section the process of creating a complete system that fulfills the project requirements and goals will be discussed. This includes an overview of the system topology, the choice of components to be used, preparations for both stationary and, during the later stages of the project, rotating testing.

3.1 System topology

In Figure 5 a simplified overview of the whole system is presented, including both the stationary and rotating sections. Worth noting is that this is considered a fully functioning realization of the system which meets the requirements presented in section 1.2, and as such may not be representative of the end product. A more in depth description of each component can be found under section 3.2 while a detailed electrical schematic of the rotating section can be found in the appendix.

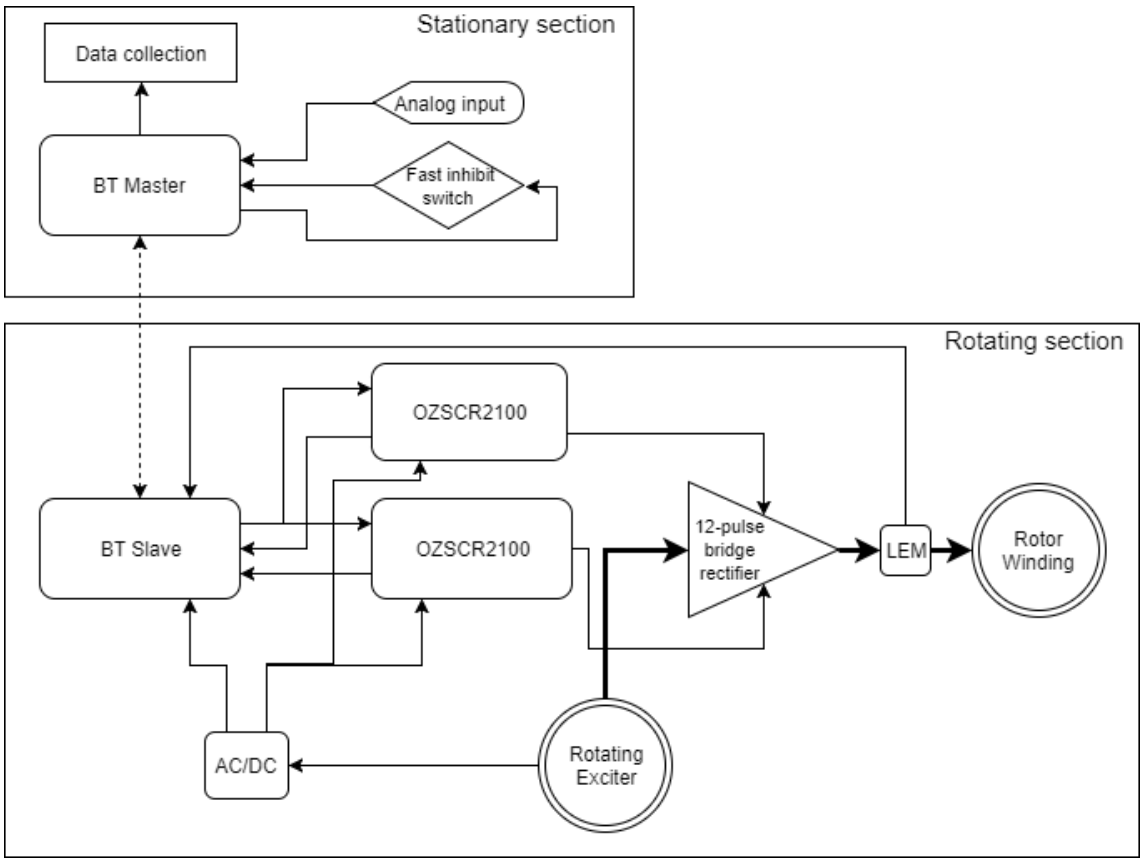

Figure 5: Simplified overview of the stationary and rotating sections. Thick lines represent high power flow.

3.2 Components

3.2.1 ILB BT ADIO MUX-OMNI

The ILB BT ADIO MUX-OMNI from Phoenix Contact is a BT device that is made for industrial use. It consists of one master and one slave and is able to transmit two analog and 16 digital signals bidirectionally.

It has an omnidirectional range between 50 to 100 meters in industry halls with the provided omnidirectional antennas and up to 400 meters outdoors with directional antennas. Although these ranges can vary depending on interferences from external sources. The signal strength is displayed on both the master and the slave device with a bar graph on the front.

Both the slave and the master needs a supply voltage between 19-30VDC with a current of 100mA. The devices does not have any supplied software but instead uses a plug and play system.[9]

3.2.2 OZSCR2100 firing board

The OZSCR2100 is part of a new generation of SCR (Silicon Controlled Rectifier) firing and control solutions from Oztek Corporation. Their purpose is to consolidate a lot of the equipment needed for rectifying an AC source and providing these in a single product.

A single board can supply firing signals to six individual thyristors and synchronize to the three AC line phases using a digital PLL (phase locked loop). After synchronization has been achieved, control of the thyristors is dictated by an analog control input signal and the mode of operation, which can be configured in the registry using Oztek Power Studio. The modes of operation are as follows:

- **Phase angle control mode**
  Direct control of the firing phase angle proportional to the analog control input signal, where the analog control input signal range defaults to 0-10 V, which in turn yields a 180-0 degree firing phase angle. This mode of operation is meant to be used when a high-level system controller is present or when wanting to manually control the rectifier output.

- **Zero cross control mode**
  Control of the number of AC line cycles in which to fire the thyristors, where the total amount of AC cycles in one "control cycle" can be specified in the registry by the user using Oztek Power Studio. As such the analog control input signal dictates how many of the total amount of cycles to fire the thyristors. For example, if the total amount were to be set to 50 then a 20% input signal would result in the thyristors being fired for 10 cycles and inhibited for 40 cycles before repeating. As with the phase angle control mode it is meant to be used together with an external system controller.

- **Closed loop DC voltage control mode**
  A self-regulating control mode of the rectified output voltage. Using this control mode utilizes the on-board regulation electronics of which the P-, I- and D-parameters, as well as min and max DC voltage values, can be specified by the user using Oztek Power Studio. Connection of the DC voltage to the board is required for measurement purposes. In this case the analog control input signal is instead used as a setpoint proportional to the min and max values.

- **Closed loop DC current control mode**
  Similar to the voltage control mode but requires the measurement of DC line current using a separate and compatible LEM style current sensor. All of the required contacts to operate the current sensor are supplied by the board which include ±15 V, signal in and ground. In this mode the analog control input signal is also used as a setpoint proportional to the min and max DC current values specified in the registry.

The board allows for a plethora of other parameters to be configured in the registry, far to many to be comprehensibly explained in this section, but some of the more important features for this project include:

- Digital I/O pin assignment
- Digital I/O polarity selection
- Line over-/under-voltage warning threshold
- Analog input pin assignment
- Analog control input signal mode
- Firing angle slew rate
- Min-/max-firing angle
- Firing pulse width

For monitoring purposes the digital I/O pin assignment will be configured to report the PLL unlocked, board fault, fast inhibit and AC line over-/under- voltage signals on pins 1 through 4.

The digital outputs does not produce any output voltage on their own but are of the type open collectors, meaning that when a digital signal is reported the pin is connected to digital ground. As such, the digital I/O polarity is configured to reverse all four outputs. By doing this one can represent the digital signal as a voltage by connecting a resistor to each port and applying a voltage to the resistor. Thus, whenever a signal is reported the pin becomes separated from digital ground and a voltage can be sensed in-between the resistor and digital output pin.

By configuring the analog control input signal mode one can specify whether to control the board using voltage or current, with the ranges available being 0-10V, 0-5V, 4-20mA and 0-20mA. For simplicity the setting used will be 0-10V. The resulting firing angle will, as previously stated, be proportional to the analog input within the specified range.

Firing of the thyristors is achieved by applying a so called "picket fence" pulse train to their gate terminals. This pulse train is visualized in figure 6 below. It is essentially a series of consecutive pulses, with configurable width and where the first one, pulse A, is of greater magnitude.

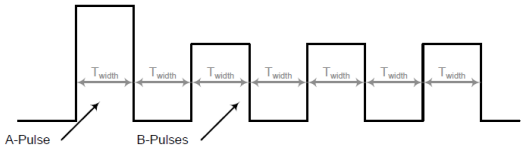

Figure 6: Picket fence pulse train. [10]

The larger first pulse ensures a full turn of the thyristor in order to lower the associated switching losses, while the following smaller B pulses are used to sustain continuous operation of the thyristor under light or discontinuous loads[10].

Furthermore, a thyristor needs to be forward biased in order for avalanche breakdown to occur, i.e. turn-ON. As the voltage across the thyristor at voltage cross-over is zero this cannot be achieved. Therefore a minimum possible firing angle can be specified in order to ensure that some voltage potential exists when the first pulse arrives at the gate terminal, thereby properly utilizing the pulse train and its function.

3.2.2.1 Oztek power studio

Oztek power studio is a graphical interface for Microsoft Windows that can modify Oztek´s power control products. There are four tabs on the front end that consists of the four main features. The names of the different tabs are “Dashboard", “Instrumentation", “Configuration", and “Software Upgrade”. The Dashboard provides the most critical information about the system such as faults, warnings and the status of the device. Instrumentation provides measurement data in more detail than on the dashboard. There are also various options to choose from and this tab can be customized to show the data needed for different types of setups. In the configuration tab viewing and modifying of configuration parameters are done. A file named Oztek Config (.ozCfg) loads all the parameters for the specified control product and shows its default-, min- and max-value for every parameter. This file can now be edited and saved for easy setup for more than one device. The software update tab is a tool for updating your software to the latest version. [11]

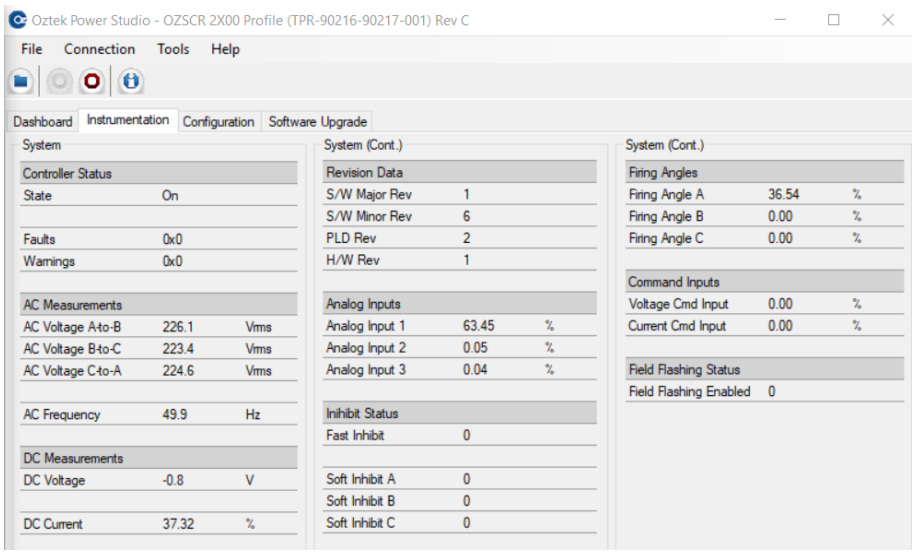

Figure 7: Oztek Power studio GUI showing the instrumentations tab.

3.2.3 Power supply unit

QUINT4-PS/1AC/24DC/5 from Phoenix Contact is the AC to DC converter that is used in this case to supply both the Oztek cards and the BT device. The input voltage range is 110-230VAC and can be connected either with a line to line connection or line to neutral with a frequency range of 50-60Hz ±10%. The DC output voltage can be set with a push of a button on the chassis to be anything between 24-29,5VDC.

For safety reasons the QUINT4-PS has a built in gas-filled surge arrester for surge protection. If the voltage gets to high, it ionizes the gas which makes it an effective conductor that connects the voltage to the ground. When the voltage goes down and reach normal levels then gas will yet again become a poor conductor and normal operations can continue. QUINT4-PS is also electronically idling-proof and short-circuit-proof and will in the event of an error limit the output voltage.[12]

3.2.4 SKKT 92 thyristor pack

SKKT 92 from Semikron consists or two thyristors in series and therefore three packs are used in fig 3 for a 6-pulse application, and six packs for the 12-pulse system. To transfer the heat from the SKKT 92 there is an aluminum oxide ceramic isolated metal baseplate on the backside of the transistor that transfers the heat to the body it is mounted on. The current ratings on this thyristor pack is somewhat over-sized for this application but had about the same price as the lower rated ones which lead to that these were chosen.

3.2.5 Peripherals

Current measurement

LEM LA 55-P is a closed loop current transducer that in this case is used to measure the DC link current on the rotor. This hall effect sensor has a conversion ratio of 1:1000. For example if the measured current is 10A then the output current will be 10mA. Since the analog inputs on the BT device responds to voltage, a measuring resistance R_m have to be added to the output. Then the voltage drop across R_m (V_m) is connected to the BT and transfered as an analog signal. One of the reasons that this type of current sensor was used is because the control cards has a built in ±15V connection for the explicit use of LEM current sensors, so no extra components were needed.

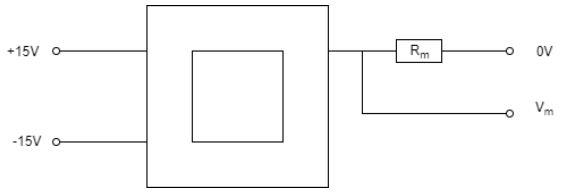

Figure 8: LEM circuit scheme.

ADXL203EB

ADXL203EB from Analog Devices [13] is a small dual axis accelerometer that can measure up to ±1.7g in each direction. Both the x- and y-outputs follows $V_{out} = V_g + 2.5$, where V_g is proportional to the sensed g-force in either direction. As such the output ranges from 0.8 to 4.2 volts, where any forces sensed outside this envelope is cut out.

It uses a built in low-pass filter with a default cutoff frequency of 50Hz that can be altered by changing the capacitors C2 and C3. The values of C2 and C3 can be calculated using Eq.4. [13]

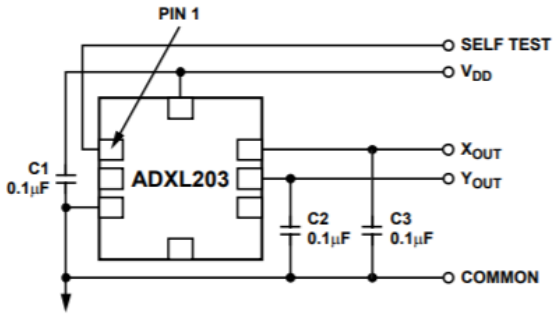

Figure 9: ADXL203EB circuit scheme.[14]

$$f_{-3dB} = \frac{1}{2\pi(32k\Omega)C_{x,y}} \tag{4}$$

For the purposes of measuring vibrations stemming from torque pulsation the sensor will be placed on the stator side of the rotating exciter. The frequency of these torque pulsations follows $F_{tp} = n_p * f_e$, where n_p is the number of pulses used in the rectification process and f_e the electrical frequency of the rectifier input phases. This results in 300Hz and 600Hz for 6- respectively 12-pulse rectification when operating at nominal frequency. As such the low-pass filters has been adjusted to include these frequencies.

3.3 Stationary tests

Stationary testing was the first step in verifying desired functionality of individual components and their compatibility with each other. By performing these tests it allowed for optimization of the system in a manner that was more time efficient than what would have been possible during the later stages of the project. Furthermore, the risk of causing damage to components due to the high g-forces and vibrations associated with rotating testing is also removed.

As the complete system will be quite complex and include several different components, testing was done incrementally, introducing and implementing components one at a time. A more in depth breakdown of this can be found in section 3.3.1 below.

3.3.1 Approach

As the system is centered around the OZSCR2100 testing started off with only using it separately, experimenting with different configurations and built in functions. Further on the OZSCR2100 was tested using a simple setup of thyristors and loads to achieve rectification of three phases utilizing a potentiometer to synthesize the analog input signal by voltage division.

An interesting aspect regarding the BT modules is their response time, as such these were also tested independently. By using a simple mechanical switch, simulating an analog pulse to be transmitted, the step response can be analyzed. For the purpose of regulating the field current using a high-level controller one has to consider the whole system response, including return of a second analog signal representing the measured current. This adds, at the very least, yet another delay caused by the BT transmission.

When having tested most of the components separately a system containing and connecting all of these together was constructed. Subsequent testing was done to merely ensure desired functionality for 6-pulse rectifying before adding a second OZSCR2100.

Testing of 12-pulse rectifying was a very important step because of the uncertainty associated with running two of the firing boards in parallel and how this would affect their behavior. In order to simulate the six-phase rotating exciter on SVANTE a transformer connected in a Wye-Delta-11 configuration was used. A visualization of such a connection can be seen in fig. 10.

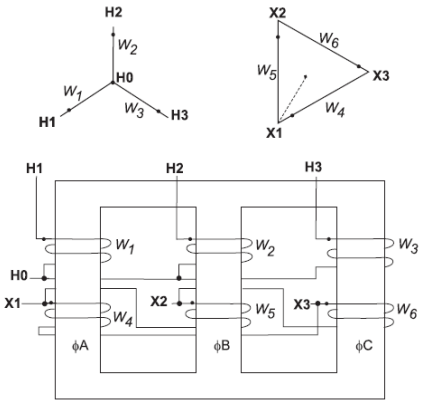

Figure 10: YD11 coupling of a transformer, yielding a 30 degree phase shift (leading) of the outputs relative to the inputs. H1, H2, H3 and H0 correspond to the three input phases and neutral line, while X1, X2 and X3 correspond to the three output phases.[15]

This effectively creates a second three-phase source which is phase shifted by 30 degrees from the original, simulating the outputs which are present on the rotating exciter in SVANTE.

Connection of the two firing boards were done in such a way that each board and associated thyristors uses its own three phases to provide half of the output power. This means that they are completely independent from each other without any master/slave configuration and that the function of the 12-pulse rectifying process relies on the fact that the upper and lower conducting thyristors will switch automatically whenever voltage cross-over happens. Which will then be twice as often compared to regular 6-pulse rectifying. The analog control signal is simply relayed to both boards without any change in amplitude or timing.

3.4 Structural enclosure and assembly

On the top of the rotor shaft there is a section that fits a structural enclosure (SE) where all the rotating components can be mounted seen in fig.1. When designing the SE there is a few factors that needs to be considered. The g-forces on the components inside the SE will scale linear with the radius of the SE. If the radius is small the risk of component breakdown is lower but the tests does not become very realistic, also there is not much room to fit all the components. With a larger radius the tests can be considered more realistic and an increased area inside the SE is accessible for more optimal solutions regarding component placement and attachment. Consultation with both Mats Wahlén at Svea Power and Urban Lundin at UU resulted in a SE with a radius of 30cm.

The drawing for the SE was done in Solid Works. Some requirement from the selected workshop had to be met regarding the k-factor of the material and bend radius to match their machines. Stainless steel became the material of choice since it is both robust and non magnetic. The final drawings, without its lid, can be seen in fig.11.

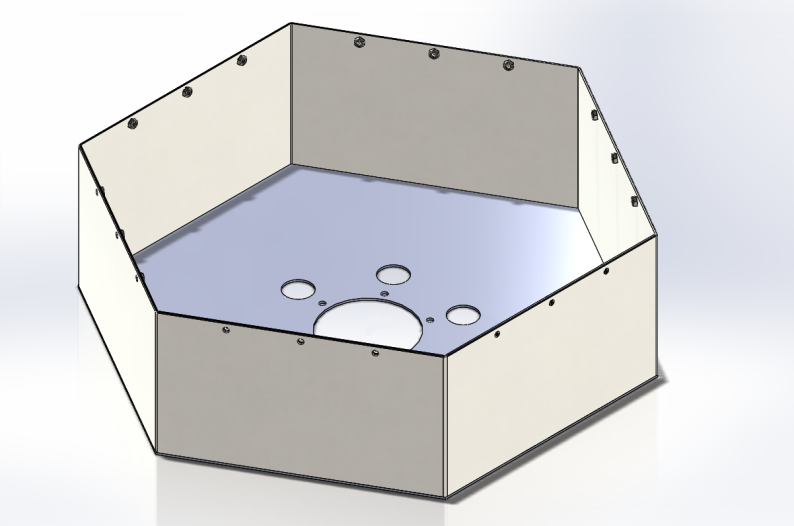

Figure 11: CAD drawing of structural enclosure.

When attaching the component in the SE one has to carefully consider where and how to do this because of the g-forces and in which direction these will act. Apart from the g-forces there were also vibrations that will require even sturdier fixtures. For more realistic results most of the components were mounted at the edges of the box to be able to test them at the maximum g-force the SE has accessible. This also minimize mechanical stresses on the fixtures since most of the g-force will act in a direction perpendicular to the edges. For the components mounted on a circuit board it is important that they get pushed into the board rather than pulled away. Therefore the position of every part had to be chosen with that in mind.

Custom-made fixture solutions had to be constructed for every part. Most of the parts were fixated with a rubber mat to both dampen vibrations and electrically isolate these form metal the surface. Then bolted to the surface with locknuts, loctite and lockwashers. To avoid unnecessary vibrations the distribution of mass within the enclosure had to be properly balanced. Therefore component of similar weight where fixated on opposite sides inside the enclosure (fig.12).

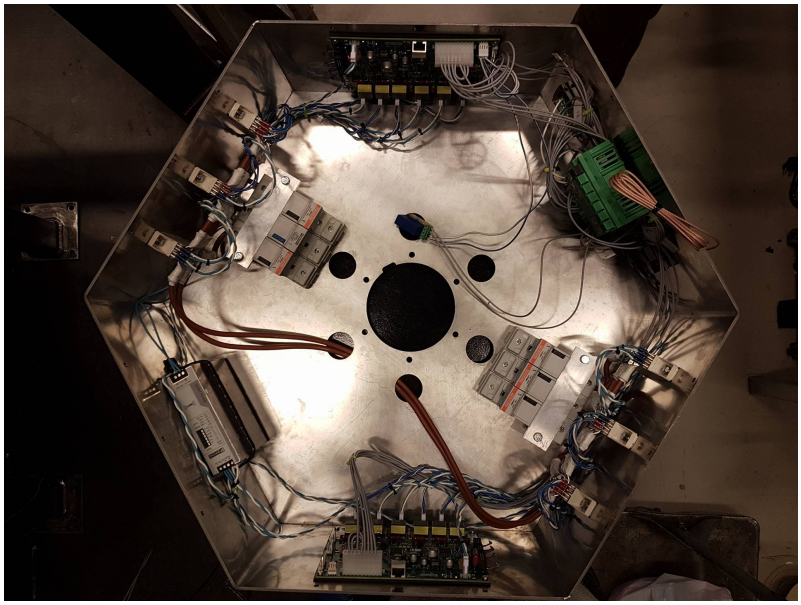

Figure 12: Top view of mounted components

3.5 Rotating tests

After having verified that the whole system operates as intended while stationary the rotating tests could finally commence. In this section the setup and preparations for rotary testing will be presented. Fig.13 shows the rotating enclosure mounted on the rotor shaft.

Figure 13: Structural enclosure mounted on the rotor shaft. Note the BT antenna protruding from the box slightly beneath the central shaft.

3.5.1 Risk management

In order to lower the risk of damaging the system before any data could been collected, the rate of rotation was increased incrementally, allowing for testing at sub-nominal frequencies.

Due to the electrical frequency and voltage being fed to the system being dependent on the mechanical rotation, the on-board PSU would not work as intended at very low speeds. As such a stationary auxiliary power source was initially used to provide the necessary voltage to power the firing boards and BT module. This was achieved using two slip rings and disconnecting the

on-board power supply. The PSU was reconnected later on when testing at higher speeds were performed.

Furthermore the output was applied to a stationary load, through yet another pair of slip rings, instead of the rotor winding. This was done in order to minimize the risk of causing harm to the generator in case of system failure during high current output. The inductance of said stationary load was measured to be ∼200mH, whereas the resistance could be varied from 2-14 Ohm in steps of 2.

3.5.2 Monitoring system functionality

System functionality had to be verified in real-time during testing and as such each firing boards was configured to send digital signals on all of their available outputs. The signals that were sent was chosen to be the PLL unlocked, fast inhibit state, board fault and line over/under voltage warning signals as these are considered relevant pertaining to overall system behavior. Whenever a signal is sent, a LED on the receiving BT module will light up and thus inform the user of its current state.

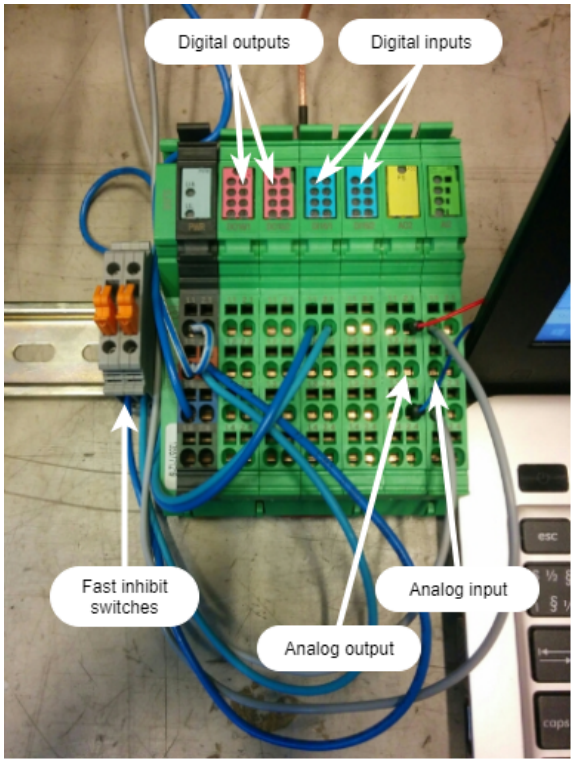

Figure 14: Bluetooth connections

As the firing boards are designed to operate nominally with an input frequency close to that of the electrical grid (50/60Hz) the digital PLL might have difficulty locking onto the input phases during lower frequencies and voltages. Therefore testing with an active output may only be done whenever the PLL is locked, which is indicated by the corresponding LED lighting up as previously stated.

Further monitoring regarding power output was done by measuring the voltage across and current through the stationary load using a voltage probe and current clamp. The current measured by the on-board LEM sensor was also sent through the BT link and received on the stationary side. These measurements are then collected using a PicoScope 4424 which allows for real time observations on a computer and easy saving of the data.

Switching between 6- and 12-pulse operation is done by sending either one or both of the signals needed to reverse the fast inhibit state otherwise present. As such this can be done during rotation without the need for accessing the firing boards using Oztek power studio.

3.5.3 Effects from torque pulsation

Vibrations caused by torque pulsation was monitored with ADXL203EB continuously during the rotating tests. The main focus for these measurements is to monitor the difference in vibrations between the 6-pulse and 12-pulse configurations. Therefore the accelerometer is mounted as close to the rotating exciter as possible since the vibrations will be more prominent in proximity to their source.

The sensor was wedged in-between two aluminum bars, used to hold the permanent magnets in place, on top of the rotating exciter stator as seen in fig.15. This allows for any tangential vibrations to be directly transferred to the sensor.

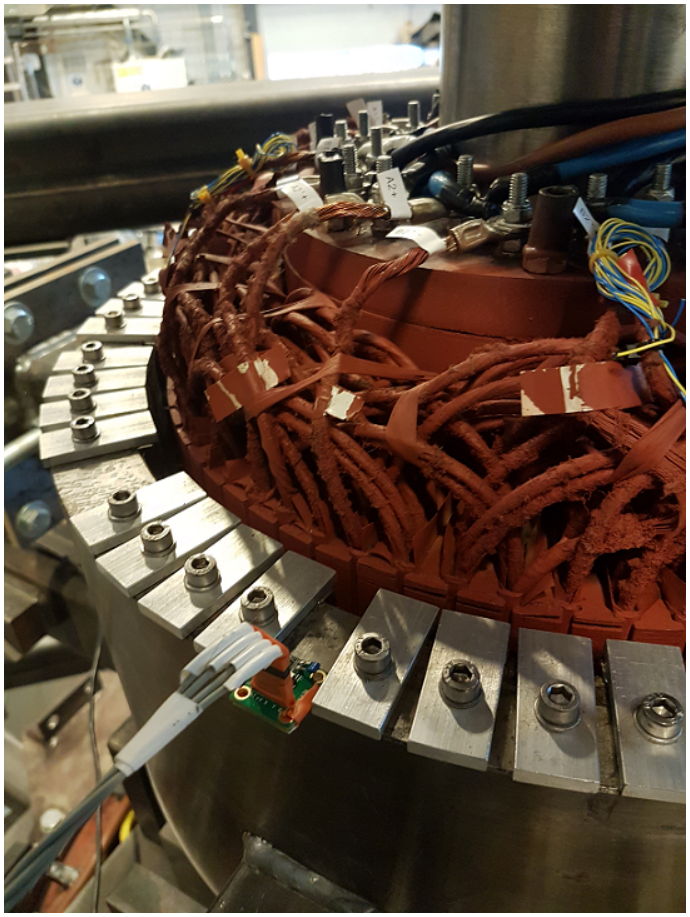

Figure 15: The ADXL203EB accelerometer in position. The copper colored section is the rotor, while the silver colored bars bolted to the stator are the aforementioned aluminum fixtures.

3.5.4 Component durability

During rotation the components are exposed to both vibrations and high g-forces. At nominal rate of rotation the g-forces applied to the components is almost 85g along the outer edge of the SE in accordance to eq. 5, where r is the radius and T the period.

$$a = w^2 \cdot r = \frac{4 \cdot \pi^2 \cdot r}{T^2} \quad [m/s^2] \tag{5}$$

It is therefore of great interest to observe the behavior of each component during and after testing. Where prolonged exposure to such an environment may be detrimental to circuitry containing electrolytic capacitors, electromechanical components, weak solder joints and silica filled fuses amongst other. Detection of any side-effects caused by the g-forces is merely done by monitoring the collected data and digital signals being received in real-time. As such any small or insignificant changes to the components during rotation might be difficult to detect.

4 Results

In this chapter a performance review of the constructed excitation system is be presented from both the stationary and the rotating tests. Results from both 6- and 12-pulse rectifying is also presented.

4.1 Stationary tests

The first tests of each component individually was done without any shortcomings and all components worked according to their data-sheets. When combining all the components successively everything worked according to plan as well.

4.1.1 System step response

To measure the total system step response a switch was used to change the analog input (signal in) from 0% to 100% instantaneously. The analog input signal was then transmitted to the firing board via bluetooth resulting in an increased load current that was measured and then transmitted back via bluetooth once again. The time it took from the switching pulse to the load current on the receiving end to reach 90% of the intended value was approximately 65ms according to fig.16. Tests has also been done with smaller changes to the analog input (0% to 10%) but the total system step response was still 65ms. The load current on the receiving end in fig.16 also shows that the bluetooth device filters the analog signal to showing more of an average value than it actually was. Both the LEM and the firing boards reacts a lot faster and can almost be neglected since the vast majority of the time delay comes from the bluetooth transmission.

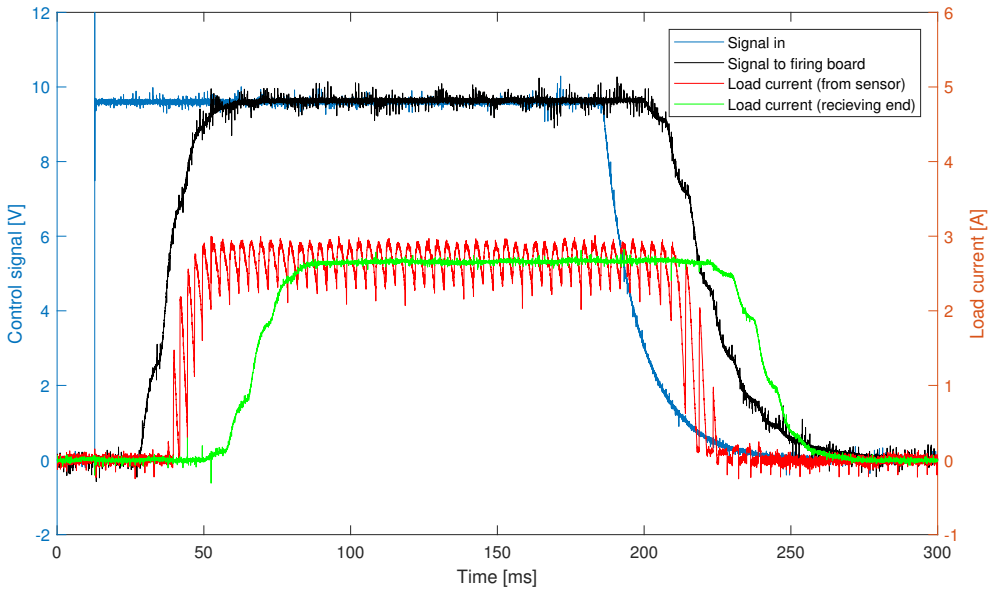

Figure 16: Total system step response.

When switching of the analog input from 100% to 0% the analog input does not drop instantaneously to 0%. This is probably due to some capacitance within the analog input on the bluetooth device being discharged over time. This can be overcome by coupling the analog input to ground when switching, allowing for a faster discharge, instead of just leaving it to float. Unfortunately this was not though of during testing and no new tests on this setup were performed.

4.1.2 Six-/Twelve-pulse system functionality

Both the six and twelve pulse tests where done with a purely resistive load and with the same firing angle of 25 degrees. The firing boards in the 12-pulse setup does not have any master-slave connection between them but instead work separate controlling three phases each. When comparing fig.17 and fig.18 the resulting current shown in black has less ripple in the 12-pulse case.

Worth noting is the slower transition of phase currents in the moment of switching when using 12-pulse compared to 6-pulse. This behavior is even more prominent at lower firing angles.

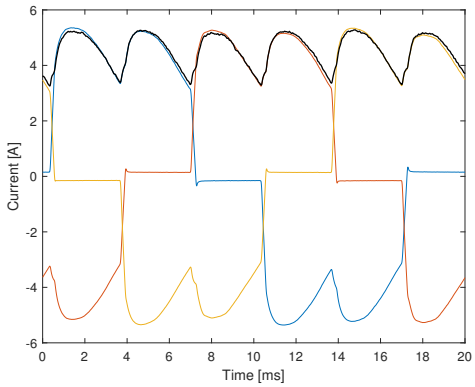

Figure 17: Phase and load currents during 6-pulse operation.

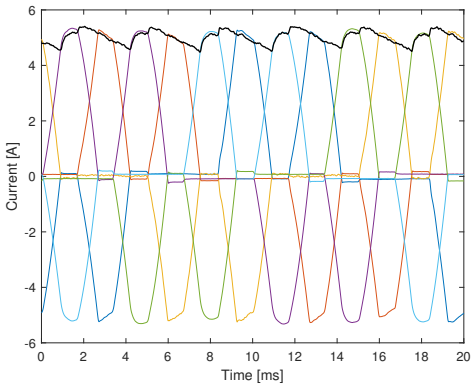

Figure 18: Phase and load currents during 12-pulse operation.

4.2 Rotating tests

4.2.1 Component durability

The speeds at which tests were done ranged from 130 to 500 RPM. During these tests no apparent problems were detected in regards to the high g-forces being applied on the components.

After the tests were done a visual inspection of the components were performed where no critical defects were detected. The thermal compound used on the thyristors had been smeared out along the inside of the box. This can be seen in fig.19 below and is due to the direction that the centripetal force is being applied on the outermost thyristors.

Figure 19: A picture on one of the outer thyristors, showing the thermal compound smeared out from its side.

The thermal compound that had been smeared out probably originates from excess amounts that had been pushed to the sides when bolting down the thyristors during assembly. However, over a longer period of time the layer in-between the thyristor and SE might be at risk of depletion, resulting in a lower thermal conductance between these.

Furthermore, slight bending of a few thyristor drive connectors on the firing boards was also observed, but not enough to be considered dangerous. All in all the total time spent rotating the system amounts to approximately one hour divided over several runs and at different speeds, with at least half of that at nominal speed.

4.2.2 System behavior

During incremental spin-up of the generator it was observed that PLL could be achieved at electrical frequencies as low as 13 Hz, allowing for operation of the system in the span of 130 to 500 RPM as previously stated. As the system proved to be capable of operating all the way up to 500 RPM, results during sub-nominal speeds will be mostly omitted.

Tests were performed using 6- and 12-pulse operation, at different firing angles and load resistances. This yielded several different cases where vibrations form torque pulsation could be observed, differing in frequency and amplitude. More on that will be presented in section 4.2.3.

Later on it was also found that the on-board PSU was powered up and able to provide power to the components when the input reached an electrical frequency of 26 Hz. Tests also showed that

the PSU could sustain supply during full 12-pulse rectifying operation of the firing boards at this threshold.

An effect of supplying the PSU using two of the input phases can be seen in fig.20. In 12-pulse operation irregularities in the output voltage during every sixth firing cycle can be seen. This effect was also observed during 6-pulse operation although not as prominently.

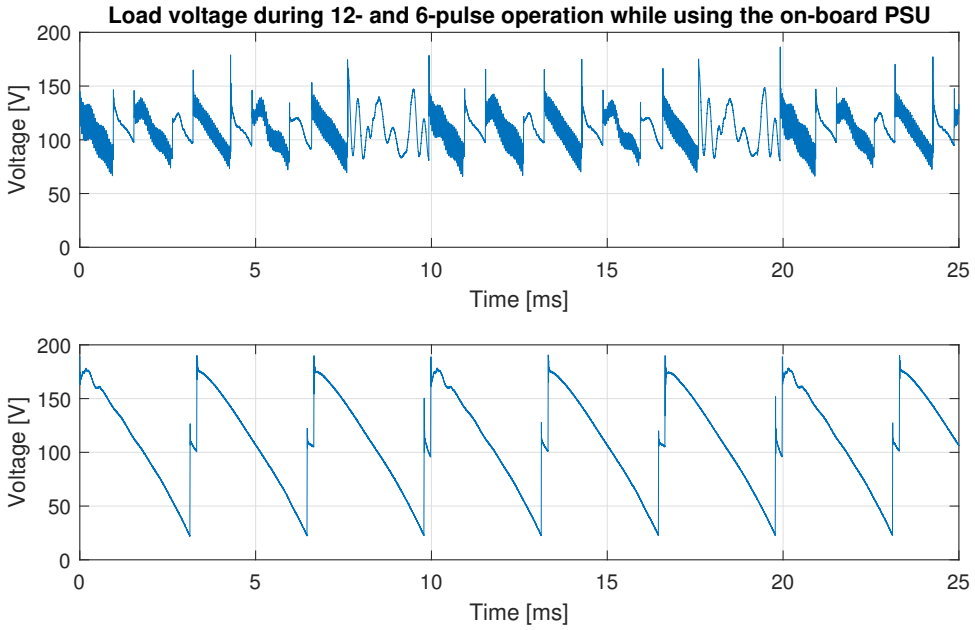

Figure 20: The first plot shows voltage irregularities during 12-pulse operation, affecting every sixth cycle. While the second plot shows the same effects every third cycle during 6-pulse operation. Both during nominal speed. The firing angle used was 63 and 50 degrees for 12- and 6-pulse respectively, this was done to match the average DC output current during both modes.

These effects were even more prominent during sub-nominal speeds, as seen in fig.21, where the line-to-line voltage was lower, thus requiring the PSU to draw a larger current in order to supply the power required by the components, increasing the voltage losses in the exciter windings.

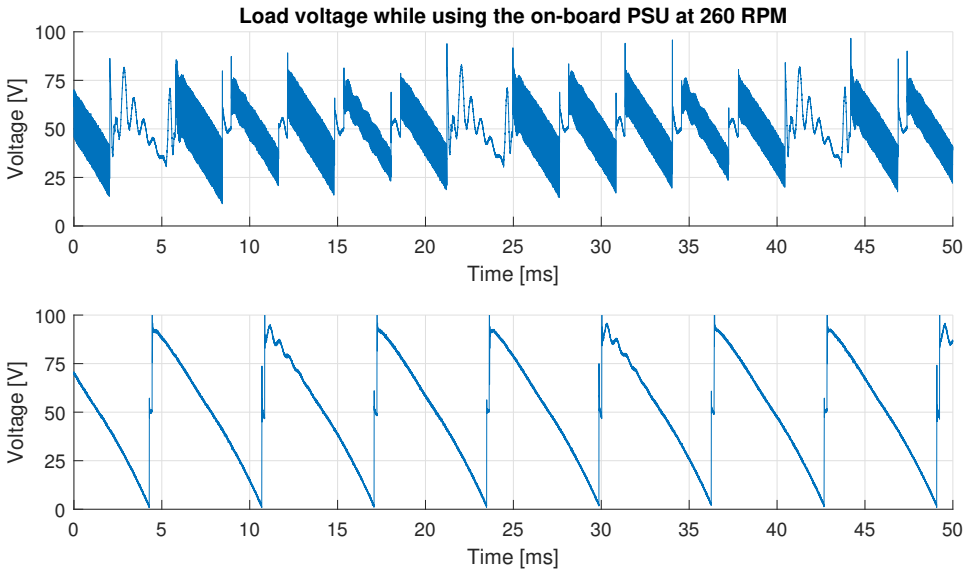

Figure 21: As in the previous figure both 12- and 6-pulse operation is presented in the figure, where the voltage irregularities can be seen in every sixth and third cycle respectively. Worth noting is that the frequencies and voltages are lower than before, therefore both the Y- and X-axes are rescaled.

On a separate note the BT communication suffered a packet loss twice during the rotating step response test shown in fig.23. Causing a slight increase in total system delay. Other than that the connection was stable during all of the tests. In regards to the response time without packet loss there is little to no change when compared to the stationary tests. The only difference would be due to the load being highly inductive, resulting in a larger rise-time of the current.

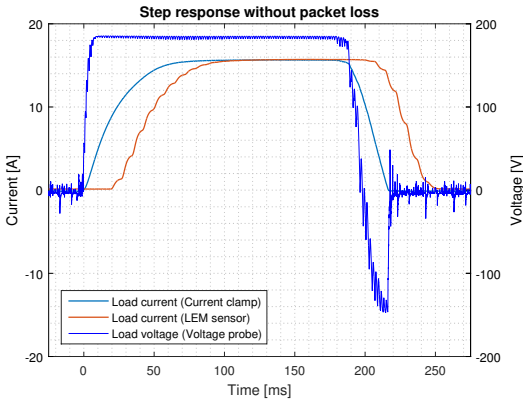

Figure 22: Step response during rotating operation. With the current rise-time equaling approximately 45 ms.

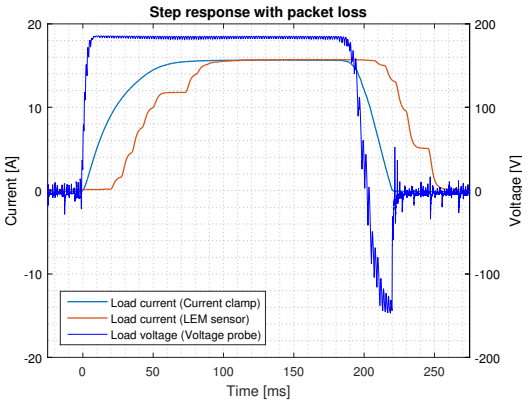

Figure 23: Step response with packet loss during both current rise and fall, increasing the rise-time to about 53 ms.

Furthermore these step responses shows that the excitation system is able to apply a negative field voltage whenever the firing angle exceeds 90 degrees, thus reversing the power flow and decreasing the field current at a faster rate than otherwise possible which can be seen in the difference between rise- and fall-time.

4.2.3 Measured vibrations from torque pulsation

The vibrations stemming from torque pulsation in the rotating exciter can be clearly seen in fig.24 below. These vibrations have an obvious correlation with the output as they are in phase with the measured load voltage. The firing angles used were 49 and 63 degrees for 6- and 12-pulse respectively. These were chosen in order to maximize the observed vibrations, simulating a worst case scenario, but also to match the output current in both cases. The load used had a resistance of 12 Ohms and an inductance of approximately 200 mH.

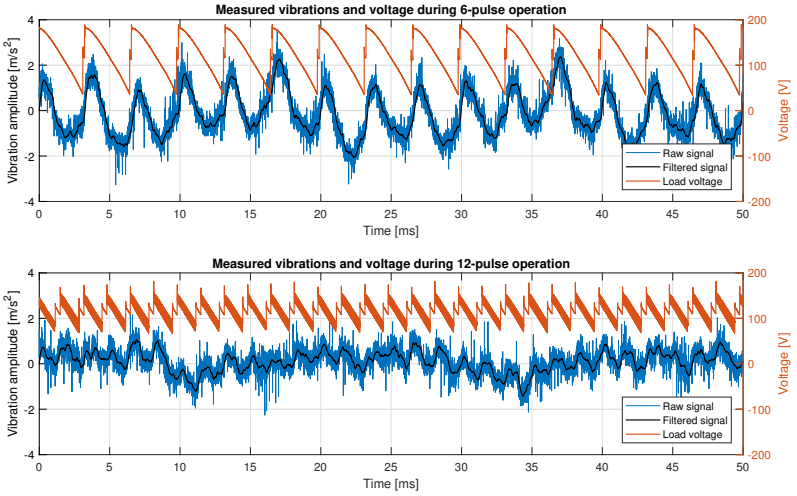

Figure 24: Showing load voltage and measured vibrations for the two cases, where the average DC output was approximately 9.7 A. The filtered vibration signal was created using a first order lowpass filter with a cutoff frequency of 1kHz.

Applying an FFT on the raw vibration signals allows for the frequency spectrum of each signal to be analyzed. The fundamental and harmonic content of each signal is clearly seen in fig.25 which confirms that the vibration frequency is tied to the electrical frequency and amount of pulses used. The fundamental components are detected at 300 and 600 Hz for 6- and 12- pulse respectively, whereas the harmonic content can be found at multiples of these frequencies.

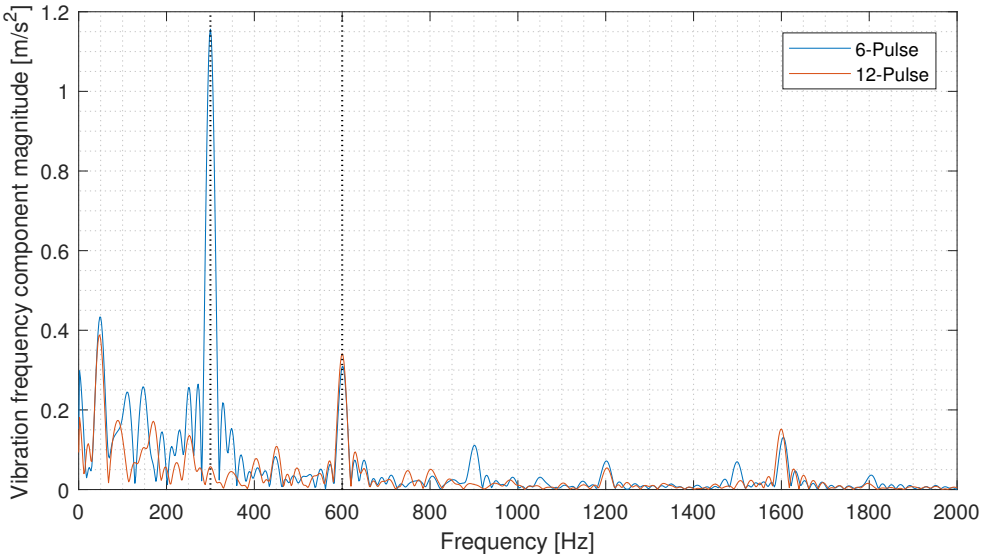

Figure 25: FFT of the unfiltered signals represented in previous figure. For reference dotted vertical lines are placed at 300 and 600 Hz respectively. Note the vibrations which can be observed at 50 and 1600 Hz. The 50 Hz component can probably be attributed to electrical interference.

In order to observe how the vibrations relates to power output another test was preformed with half the resistive load, resulting in twice the load current. The inductive load was kept the same in both cases. Applied firing angles were also kept the same. When comparing the vibrations from the 6-pulse cases the amplitude have roughly doubled with the higher load current, while in the 12-pulse case the vibrations only increased slightly.

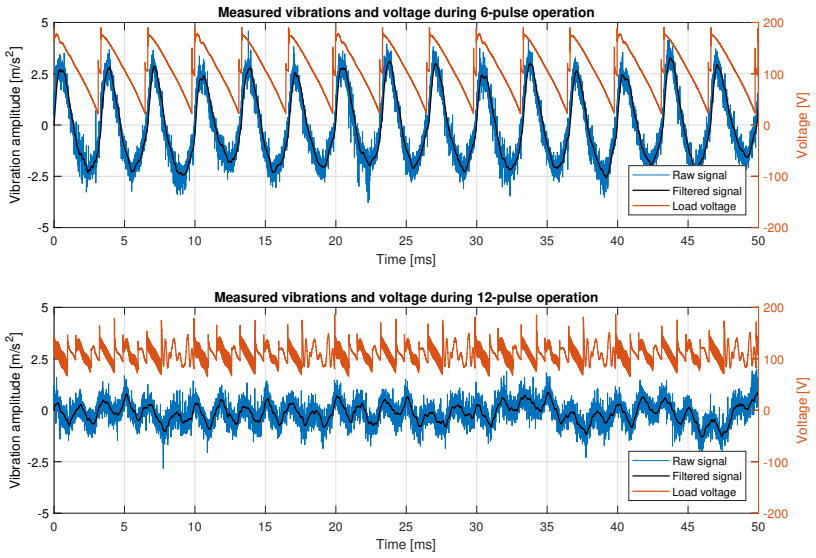

Figure 26: Load voltages and vibrations in both 6- and 12-pulse mode during the second session. Note that the on-board PSU is in use this time around, which explains the irregularities seen in the voltages.

When having increased current output, the vibrations caused while running 6-pulse became audible. This was also the case when operating at sub-nominal frequencies, requiring even less current output before being perceived.

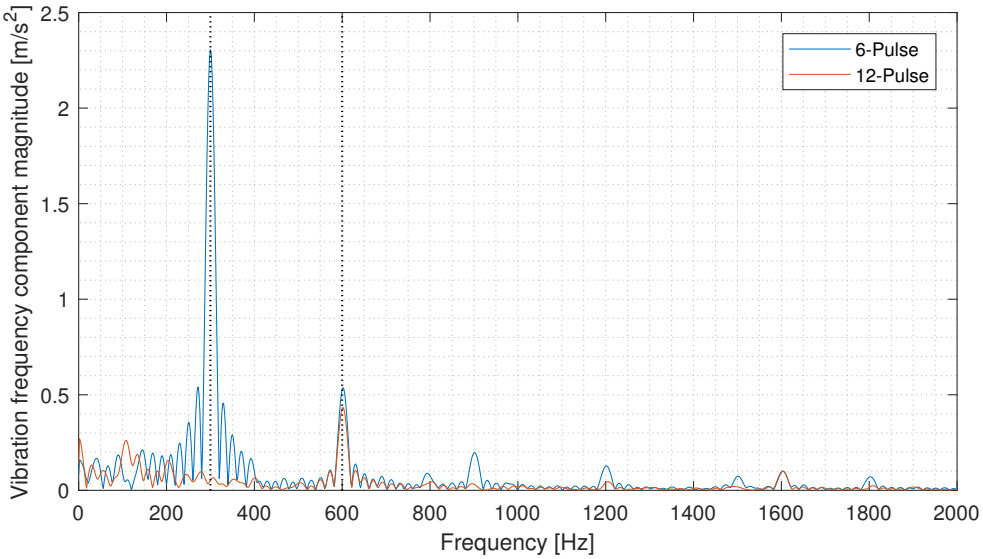

Figure 27: FFT of the unfiltered vibration signals during the second session where a higher current output was applied to the load. The dotted vertical lines are once again placed at 300 and 600 Hz.

The spectrum above clearly shows the previously stated increase in vibration magnitude, of both fundamental and harmonic content, during 6-pulse operation at higher current output. With its first harmonic even exceeding the magnitude of the fundamental component during 12-pulse rectification. Also seen is a decrease, or almost complete removal, of the interference previously present at 50 Hz. While the component at 1600 Hz is still present although slightly smaller than before.

In table 2 the magnitude of the fundamental frequency components is compared between 6- and 12-pulse rectifying during both sessions. Keep in mind that power output from the rotating exciter was roughly doubled in the second session.

	Pulse mode		
	6-P	12-P	Change
Session 1	1.16	0.34	-71%
Session 2	2.31	0.43	-81%
Change	+99%	+26%	

Table 2: Comparative table showing the different fundamental frequency component magnitudes during 6- and 12-pulse rectifying in both of the testing sessions. The magnitudes have been extracted directly from previously presented the FFT data and are still in m/s^2.

For comparison of vibrations at different firing angles further tests were performed during the first session but with lower firing angles. In fig.28 measurements of voltage and vibrations, while applying a 5 degree firing angle, are presented. It shows a clear decrease in vibration amplitude during both rectifying configurations compared to those observed in fig.24, where the fundamental frequency component magnitudes amount to 0.75 and 0.13 m/s^2 for 6- and 12-pulse respectively. Thus it proves advantageous to operate the rectifier at very low firing angles in regards to torque pulsation and associated vibrations.

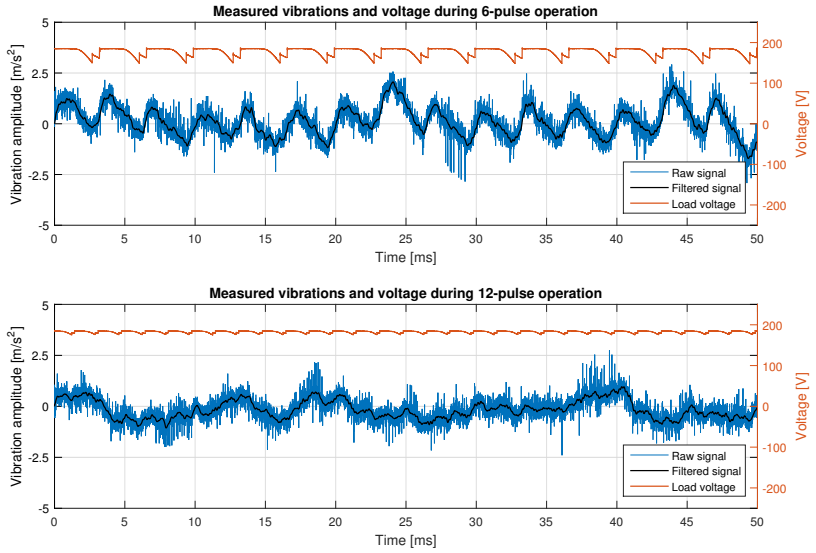

Figure 28: Output voltages and resulting torque vibrations during 6- and 12-pulse mode using a 5 degree firing angle at nominal rate of rotation.

5 Discussion and conclusions

Overall the system functioned as intended and all our goals stated in the project description were met. The firing boards where able to operate in parallel and independently of each other, effectively yielding 12-pulse rectifying from two 6-pulse systems. The bluetooth modules transmitted the signals without any major interferences or loss in communication, although two packages were observed to be lost once during the rotating step response tests. The system was shown to be operational at frequencies below nominal, where the power supply limits the lowest possible frequency to 26 Hz. With the use of an auxiliary power supply this could be lowered even further down to 13 Hz, before the firing boards lost PLL.

As for any system that is supposed to operate in an harsh environment, it is difficult to make a good estimation for how long the system would remain functional. In this project testing was done on component survivability towards g-forces for about an hour. Where commercial applicability of this system would require it to run for a considerably longer time. Therefore there is an uncertainty associated with the system durability during a longer timespan even though it did not show any unwanted behavior during the performed tests.

Heat transfer from the thyristors could become a problem when operating on higher currents for a longer time period. Especially considering that the thermal compound was displaced during rotation, risking depletion of the thin layer in-between the thyristor and SE. This risk could be mitigated with the use of a thermal compound that cures and stays in place or thermal press pads.

No tests have been done connecting the system to a high level controller. If such a controller requires measured current and/or voltage on the rotating side as feedback, time delay imposed by the bluetooth link might become an issue.

In regards to the measured vibrations caused by torque pulsation in the rotating exciter we can only determine whether these increase or decrease during different scenarios. As the sensor is placed on the static side, which in itself is fixed to the surrounding structures, calculation/approximation of the actual torque variations using these measurements would be difficult. These measurements does however support the claim that torque pulsation is lowered when operating in 12-pulse mode compared to 6-pulse.

Regarding the 1600Hz vibrations no certain source have been found, although it is possible that it originates from the gearbox driving the rotor. Furthermore, the vibration component observed at 50Hz during some of the tests can probably be attributed to electrical interference as these were only present at seemingly random times.

6 Future work

In this section a few suggestions on further studies and improvements to the system is presented. It is by no means an exhaustive list but covers some of what we considered to be the more important parts throughout the course of this project.

- Further testing on the components resilience towards g-forces and possibly even higher g-forces as well to ensure that the system performs as intended for a longer period of time.
- The vibrations could be measured on the rotating side of the rotating exciter instead of on the stationary side as done in this study. If the sensor were to be placed on the rotor, and transmission of the data could be solved, one would be able to calculate the torque pulsation as the rotor is of known mass and rotates freely from the surrounding structure.
- Testing using a high level controller to ensure proper functionality even with the time delay imposed by the bluetooth transmission. If the time delay causes problems a new bluetooth device that have a lower latency and/or shorter rise-time could possibly solve this problem.
- The PSU restricts operation to electrical frequencies above 26 Hz which could be problematic during startup of the generator. If this is the case, replacing the PSU for one that can operate at even lower frequencies should be considered.

References

[1] M. Wallin. *Measurement and modelling of unbalanced magnetic pull in hydropower generators*. 2013. ISSN 1651-6214; 1029.

[2] S. J. Chapman. *Electric Machinery Fundementals*. 2011, 5th Edition, Chapter 4, pp. 191-270.

[3] J. K. Nøland, F. Evestedt, J.J. Pérez-Loya, J.Abrahamsson and U.Lundin. *Comparison of thyristor controlled rectification topologies for a six-phase rotating brushless permanent magnet exciter*. IEEE Trans. on Energy Convers., Oct. 2015.

[4] J. K. Nøland. *A New Paradigm for Large Brushless Hydrogenerators*. Doc. thesis, Div. Elect., Ångström Lab., Uppsala Univ., Uppsala, Sweden, 2017.

[5] T. R. Kuphaldt. *Lessons in electric circuits*. 2009, Vol. 3, 5th Edition, pp. 319-356.

[6] C. Bisdikian. *An overview of the Bluetooth wireless technology*. IEEE Communications Magazine, Vol. 39, Issue 12, Dec. 2001, pp. 86-94.

[7] Bluetooth SIG, Inc. *Specification of the bluetooth system*. Core Pack. Ver. 4.0, June 2010, pp. 17-23. Available at: `https://www.bluetooth.com/specifications/bluetooth-core-specification/legacy-specifications`. [Accessed 04 Jan 2018].

[8] Emetor AB. *Torque ripple*. Web page. Available at: `http://www.emetor.org/glossary/torque-ripple/`. [Accessed 27 Nov 2017].

[9] Phoenix Contact. *ILB BT ADIO MUX*. Data sheet, Apr. 2017. Available at: `https://www.phoenixcontact.com/online/portal/us?uri=pxc-oc-itemdetail:pid=2884208`. [Accessed 04 Jan 2018].

[10] J. Goodell, Oztek Corp. *SCR Driver Board Firing Pulses*. Blog post, Apr. 2011. Available at: `http://www.oztekcorp.com/blog/bid/47387/SCR-Driver-Board-Firing-Pulses`. [Accessed 04 Jan 2018].

[11] Oztek Corp. *Oztek Power Studio User's Manual UM-0052*. Rev. D, September 2016. Available at: `http://cdn2.hubspot.net/hubfs/23453/2016_Brochures_Product_Sheets/UM-0052_Oztek_Power_Studio.pdf`. [Accessed 04 Jan 2018].

[12] Phoenix Contact. *PSU QUINT4-PS/1AC/24DC/5*. Datasheet, Aug. 2016. Availabel at: `https://www.phoenixcontact.com/online/portal/pi?uri=pxc-oc-itemdetail:pid=2904600&library=pien&tab=1`. [Accessed 28 Jan 2018].

[13] Analog Devices. *PSU QUINT4-PS/1AC/24DC/5*. Datasheet, Rev. E, 2014. Availabel at: `http://www.analog.com/media/en/technical-documentation/data-sheets/ADXL103_203.pdf`. [Accessed 04 Jan 2018].

[14] Analog Devices. *ADXL203EB Dual Axis Accelerometer Evaluation Board*. Rev. 0, 2004. Available at: `http://www.analog.com/media/cn/technical-documentation/evaluation-documentation/535395787ADXL203EB_0.pdf`. [Accessed 04 Jan 2018].

[15] L. Lawhead, R. Hamilton, J. Horak. *Three Phase Transformer Winding Configurations and Differential Relay Compensation*. Basler Electric Company, 60th Georgian Tech Prot. Relay Con., May 2006, pp. 15.

Appendix

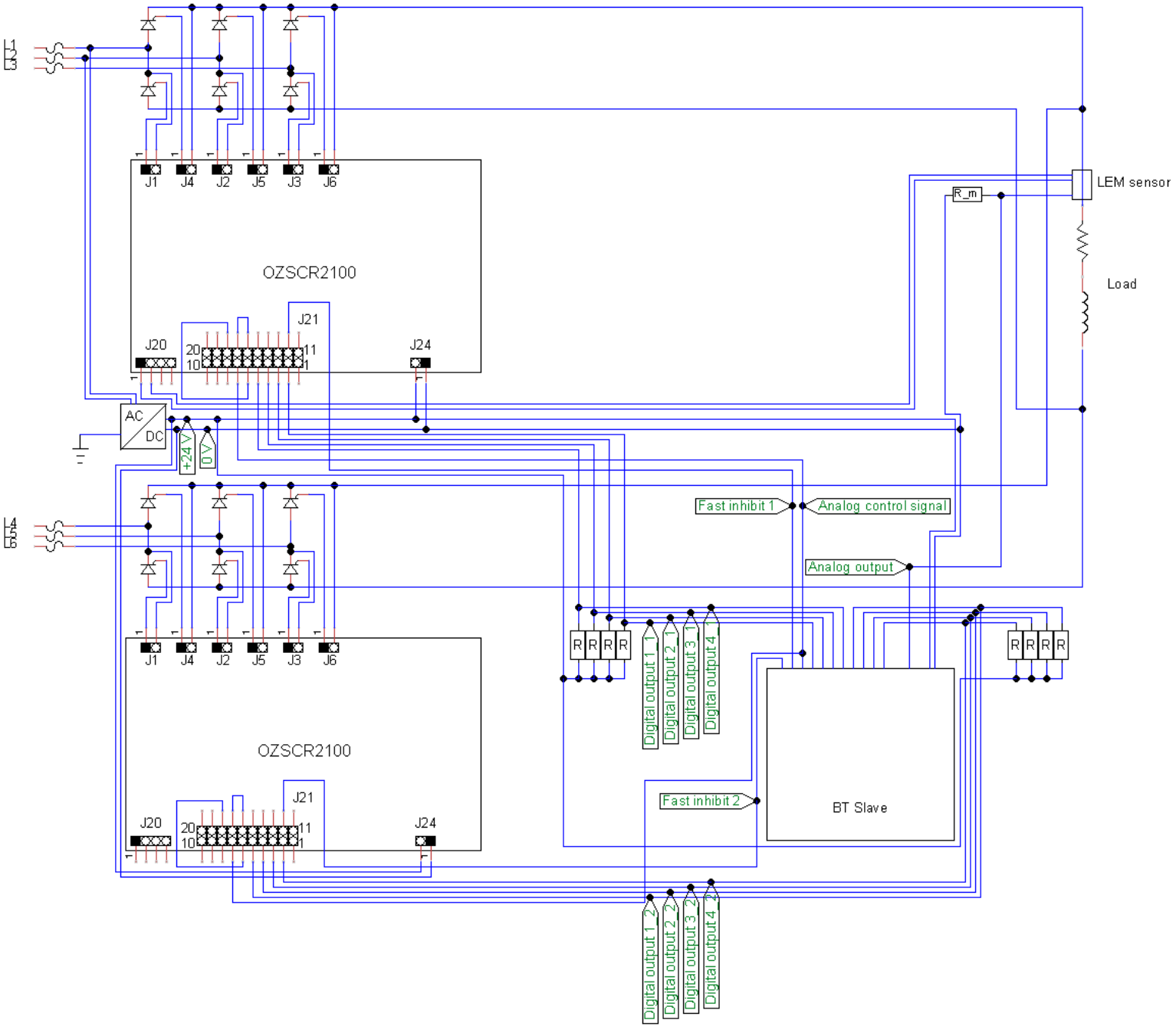

Figure 29: Electrical diagram of wiring and components present on the rotating side.